Exact Spectral Moments and Differentiability of the Weierstrass-Mandelbrot Fractal Function

Itzhak Green
GWW School of Mechanical Engineering
Georgia Institute of Technology
itzhak.green@me.gatech.edu

Abstract

Fractal mathematics using the Weierstrass-Mandelbrot (WM) function has spread to many fields of science and engineering. One of these is the fractal characterization of rough surfaces, which has gained ample acceptance in the area of contact mechanics. That is, a single mathematical expression (the WM function) contains characteristics that mimic the appearance of roughness. Moreover, the "roughness" is "similar" across large dimension scales ranging from macro to nano. The field of contact mechanics is largely divided into two schools of thought: (1) the roughness of real surfaces is essentially random, for which stochastic treatment is appropriate, and (2) surface roughness can be reduced to fractal mathematics, using fractal parameters. Under certain mathematical constraints, the WM function is either stochastic or deterministic. The latter has the appeal that it contains no randomness, so fractal mathematics may offer closed-form solutions. Spectral moments of rough surfaces still apply to both approaches, as these represent physical metrology properties of the surface standard deviation, slope, and curvature. In essence spectral moments provide a means of data reduction so that other physical processes can subsequently be applied. It is well known, for example, that the contact model of rough surfaces, by Greenwood and Williamson (GW), depends on parameters that are direct outcomes of these moments. Despite the vast amount of publications on the Weierstrass-Mandelbrot (WM) function dedicated to surfaces, two papers stand out as originators, where the others mostly rework their results. These two papers, however, contain some omissions and approximations that may lead to gross errors in the estimation of the spectral moments. The current work revisits these papers, adds information, but departs in the mathematical treatment to derive exact expressions for the said moments. Moreover, it is said the WM function is non-differential. That is also revisited herein, as another approach to derive the spectral moments depends on such derivatives. First, the complete mathematical treatment of the WM function is made, then the spectral moments are derived to yield exact forms, and lastly, examples are given where the physical meanings of the approximate and exact moments are discussed and their values compared. Numerical procedures will be introduced for both, and the effectiveness of the computational effort is discussed. One numerical procedure is particularly effective for any digitized signal, whether that originates from analytical functions (e.g., WM) or real surface measurements.

Contents

1. Introduction – Theoretical Background

Often in tribology, surfaces roughness is characterized by the spectral moments, m_0, m_2, and m_4, which respectively are measures of the variance, slop, and curvature. They are completely sufficient to execute, for example, the Greenwood and Williamson (GW) contact model [1] under elastic conditions, and other models under elasto-plastic conditions. The work by McCool [2,3], for example, provides a complete mathematical procedure on how to convert two surfaces having two-dimensional, orthotropic roughness, into a single surface having a composite roughness described by a single set of m_0, m_2, and m_4.

Evidently, however, these moments are not just specific to modeling surface roughness in tribology, as they are central in the many fields of science and engineering that fall generally into the category of signal processing for which there is ample literature (see notably the classical texts by Bendat and Piersol [4–6]). Non-tribological examples can range from the geomechanics of rough wall fracture [7] to signal processing performed on the output from the pulsed laser photoacoustic instrument monitoring crude oil in water [8], or to the analysis performed in an optical telescope [9]. Because of their general importance, the spectral moments are focal in this work.

In that framework, the work by Majumdar and Tien [10] postulates that the Weierstrass-Mandelbrot (WM) function can be "…used to simulate deterministically rough surfaces which exhibit statistical resemblance to real surfaces." They obtain the spectral moments using the power spectrum derived by Berry and Lewis [11]. Hence, these two works are central herein. However, because the spectral moments as given in [10] are derived based upon an "approximate" power spectrum that is given in [11], they can only be considered as "approximations." Their moments will be compared against the exact moments, which are derived herein.

Following [10], the WM function is:

$$z(x) = G^{(D-1)} \sum_{n=n_1}^{n_2} \frac{\cos\left(2\pi\gamma^n x\right)}{\gamma^{(2-D)n}} \quad 1 < D < 2, \quad \gamma > 1 \tag{1}$$

where n_1 is finite, and $n_2 \to \infty$. The leading constant, G, is sometimes referred to as the fractal roughness, D is a fractal dimension, and γ determines the density of the spectrum and the progressive amplitude change between the spectral modes. While both D and γ are dimensionless, γ^n must possess units to offset the units of the variable x. Since Eq. (1) uses x as a

length coordinate, the SI units inferred upon γ^n are *cycles/m*. In contrast, Berry and Lewis [11] use time, *t,* as it is relevant to the topic of quantum physics. In their representation[1]:

$$z(\text{t}) = G^{(D-1)} \sum_{n=n_1}^{n_2} \frac{\cos\left(\gamma^n t\right)}{\gamma^{(2-D)n}} \quad 1 < D < 2, \quad \gamma > 1 \tag{2}$$

where $n_1 \rightarrow -\infty$, and $n_2 \rightarrow \infty$. While a negative n_1 may be related to negative frequencies, the current work limits n_1 to non-negative values pertaining to rough surfaces. Also discussed in [11] is a phase that if made random, the WM function is stochastic, but otherwise it is deterministic. Specifically Ref. [11] uses a zero phase for the various examples and derivations, effectively rendering Eq. (2) to be deterministic. The same is assumed in the current work. In Eq. (2), γ^n must carry units of rad/s, so evidently the units of γ^n depend on the context. Either representation, Eq. (1) or Eq. (2), can obviously be represented by a single equation,

$$z(x) = G^{(D-1)} \sum_{n=n_1}^{n_2} \frac{\cos\left[(2\pi)^q \gamma^n x\right]}{\gamma^{(2-D)n}} \quad 1 < D < 2, \quad \gamma > 1; \quad q = 0 \text{ or } 1 \tag{3}$$

The switch q stipulates the meaning of units. To assess its meaning, suppose that γ^n is replaced with $\gamma_o \gamma^n$. Suppose then that γ_o carries units of say, *rad/s, cycles/m*, etc., which appropriately offset the units of *x*, however, the magnitude of γ_o is always $|\gamma_o| = 1$. Hence, γ, being unitless itself, can serve as the common ratio in the geometric progression of frequencies, γ^n, in the argument of the harmonic term. However, because $|\gamma_o| = 1$, it is superfluous to include it in the equations, so it is omitted. But the units remain, and they are imparted upon γ^n. So, if the units of *x* in Eq. (3) are either in meters or seconds, then $q=1$ imparts upon γ^n the meaning of frequency, *f,* either in units of *cycles/m* or *Hz*, while $q=0$ imparts upon γ^n the meaning of angular frequency, ω, in units of *rad/m* or *rad/s* (see below[2]). While that may seem cumbersome or just semantics, careless mix-up of units may greatly affect the calculation of the spectral moments. Hence, the meaning of the units of γ^n may be perceived by context. In addition, as the sum implies, the harmonic term is modulated by amplitudes $\gamma^{(D-2)n}$ that decrease exponentially with *n.* Before continuing, it should be noted that the leading term of $G^{(D-1)}$ is constant, and is intended to provide a global scale of interest. Otherwise, it has no role in the mathematical behavior or characteristics of the WM function (e.g., Ref. [11] omits it entirely).

---

[1] The leading coefficient, $G^{(D-1)}$, is missing in Ref. [11] but it is added here for completion. By assigning $G=1$ we comply identically with [11].

[2] Terminology-wise, when *x* is a length coordinate, and $\omega = 2\pi f = 2\pi / \lambda$, then ω is the angular wavenumber, *f* is the wavenumber, and λ is the wavelength (along *x*).

Two methods are recognized for the calculation of the spectral moments. One method is formulated in the spectral domain using the autocorrelation of the surface profile or function, followed by its power spectrum, the other is formulated in the spatial or temporal domains using derivatives of the said surface with respect to *x*. A widespread notion about the WM function, however, presumes that it is "non-differential." Because the spectral domain formulation does not use nor involve derivatives of any kind, the spectral moments are thence derived first in the spectral domain to yield *exact* forms (which counter previous work that hinges upon an *approximate* form of the power spectrum, consequently rendering inexact and largely erroneous results). Then, venturing to undertake derivatives of the WM function under the practical requirement, and condition, where the WM function is truncated, it is demonstrated that the spectral moments obtained in the spatial or temporal domains using said derivatives, *indistinguishably* match the *exact* results obtained from the spectral domain formulation. This finding may well dispel the sweeping notion that the WM is non-differential.

Also, in this work, numerical procedures are introduced along with coding scripts used for corroboration of the said analyses. The effectiveness of the computational efforts is likewise discussed. One numerical procedure particularly stands out to optimally process any digitized signal, whether that originates from analytical functions (e.g., WM) or measurements of real surfaces.

2. Calculation of the spectral moments in the spectral domain

The power spectrum method is propounded in works [2,3,10]. Using the power spectrum $P(\omega)$ of the waveform $z(x)$, yields the kth spectral moment according to

$$m_k = \int_0^\infty \omega^k P(\omega) d\omega \quad @ \; k = 0, 2, 4 \tag{4}$$

Note that for $k=0$, Eq. (4) signifies Parseval's theorem. For additional information see [7–9,12].

2.1 Previous work

The work by Majumdar and Tien [10] faithfully adopts the work by Berry and Lewis [11]. Both provide the foundation for this section (but there will be a departure, as detailed in the next section). The autocorrelation $R(\tau)$ of the WM function is

$$R(\tau) = \lim_{L \to \infty} \frac{1}{L} \int_0^L z(x) z(x + \tau) dx = \frac{G^{2(D-1)}}{2} \sum_{n=n1}^{\infty} \frac{\cos\left[(2\pi)^q \gamma^n \tau\right]}{\gamma^{(4-2D)n}} \tag{5}$$

For the sake of notation simplicity, in the forgoing of this section the switch $q=0$ is implied. A distinction will be made appropriately at the end of the derivation.

As stated by Berry and Lewis [11], the power spectrum is proportional to the Fourier transform of the autocorrelation. Equation (17) given in Ref. [11], is adopted by Majumdar and Tien [10]

(see their Eq. (4)). That equation gives the power spectrum for the WM function (adding herein the missing term, $G^{2(D-1)}/2$)

$$P(\omega) = \frac{G^{2(D-1)}}{2} \sum_{n=n1}^{n_2 \to \infty} \frac{\delta(\omega - \gamma^n)}{\gamma^{(4-2D)n}} \qquad (6)$$

where $\delta(*)$ is the Dirac-delta function. Note that in Ref. [11], the implied switch is also $q=0$. This is where Berry and Lewis [11] *approximate* the discrete and exact power spectrum of Eq. (6) by a continuous one,

$$\overline{P}(\omega) = \frac{G^{2(D-1)}}{2\ln\gamma} \frac{1}{\omega^{(5-2D)n}} \qquad (7)$$

Majumdar and Tien [10] then use this Eq. (7) in the above definition of Eq. (4), yielding the spectral moments as given by Eqs. (6-8) in their work. Those are reworked herein and combined into a single expression

$$m_k = \frac{G^{2(D-1)}\left(\omega_l^4 \omega_h^{2D+k} - \omega_h^4 \omega_l^{2D+k}\right)}{2\ln\gamma(2D+k-4)\,\omega_h^4 \omega_l^4} \quad @\, k = 0,2,4 \qquad (8)$$

As explained in [10] the angular frequencies of low and high, ω_l and ω_h, are respectively connected to the values of n_1, and n_2, and to the *practical* considerations of the largest and smallest scales of interest. For a given γ, these are

$$\begin{aligned} \omega_l &= 2\pi f_l \quad @ \quad f_l = \gamma^{n_1} \\ \omega_h &= 2\pi f_h \quad @ \quad f_h = \gamma^{n_2} \end{aligned} \qquad (9)$$

It is immediately apparent from Eqs. (8) and (9) that for a *given* set of G, D, and γ, the spectral moments shall yield *very different* values for m_k depending just on how n_1 and n_2 are assigned. It is also apparent (and noted in Ref. [10]) that for the common case where $\omega_l \ll \omega_h$, m_0 is dominated by ω_l (and thus by n_1), while m_2 and m_4 are dominated by ω_h (and thus by n_2). That behavior shall be realized in the following sections as well. It is *emphasized* that Eq. (8) is *not* an *exact* representation of the spectral moments, because it is based upon an "*approximation*" of the spectral power, particularly Eq. (7). In fact, Eq. (8) renders results that are *utterly different* from the exact answers, sometimes by orders of magnitude, as it is demonstrated later.

2.2 The exact derivation of the spectral moments

The approximation of the power spectrum that is discussed above (and given by Eq. (7)), is in fact *not* needed for the exact derivation of the spectral moments. Substituting Eq. (6) in Eq. (4) gives

6

$$m_k = \int_0^\infty \omega^k P(\omega) d\omega = \frac{G^{2(D-1)}}{2} \sum_{n=n_1}^{n_2} \int_0^\infty \frac{\omega^k \delta(\omega - \gamma^n)}{\gamma^{(4-2D)n}} d\omega \quad @ \, k = 0, 2, 4 \qquad (10)$$

after swapping the summation and the integration. While in Eq. (6) $n_2 \to \infty$, the following is valid for any n_2, *finite* or *not*. The next step is to use the sifting property of the Dirac-delta function, which, for a continuous function $f(t)$, is:

$$\int_0^\infty f(t) \delta(t-a) dt = f(a) \quad @ \, a \geq 0$$

Thus, it is readily apparent that for the switch $q=0$ (i.e., γ^n has the meaning of angular frequency in *rad/m*), Eq. (10) reduces to

$$m_k = \frac{G^{2(D-1)}}{2} \sum_{n=n_1}^{\infty} \frac{\left(\gamma^n\right)^k}{\gamma^{(4-2D)n}} = \frac{G^{2(D-1)}}{2} \sum_{n=n_1}^{n_2} \gamma^{(k+2D-4)n} \quad @ \, k = 0, 2, 4 \qquad (11)$$

Including now the switch q, we have

$$m_k = \frac{G^{2(D-1)}}{2} \sum_{n=n_1}^{\infty} \frac{\left[(2\pi)^q \gamma^n\right]^k}{\gamma^{(4-2D)n}} = \frac{G^{2(D-1)}}{2} (2\pi)^{qk} \sum_{n=n_1}^{n_2} \gamma^{(k+2D-4)n} \quad @ \, k = 0, 2, 4; \; q = 0 \, or \, 1 \qquad (12)$$

These are the *exact* spectral moments for the Weierstrass fractal function. Note that while Eq. (12) is free of x, or the signal length, it originates with Eq. (5), so Eq. (12) is derived essentially for a signal length, $L \to \infty$. That equation is straightforwardly calculated, and is offered analytically once G, D, γ, n_1, and n_2 are set. The next line of code implements Eq. (12) using a Mathematica function, e.g., for $q=1$ (i.e., γ^n has the meaning of linear frequency in *cycles/m*)

$$m[k\_] := \left(G^\wedge(2*D-2)/2\right)*(2*Pi)^\wedge k * Sum\left[g^\wedge((k+2*D-4)*n), \{n, n1, n2\}\right] \qquad (13)$$

where g is conveniently used in coding to represent, γ (that code is afterwards used to produce results in Table 1). Clearly for $k=0$, the sum in Eq. (12) converges to a finite value for m_0. However, when $k=2$, or 4, the sums for both m_2 and m_4, diverge to infinity when $n_2 \to \infty$. For the same practical reasons discussed above, n_2 must be truncated so that $n_2 = finite$. Under such conditions, again, m_0 converges, but m_2 and m_4 render finite values that monotonically and hastily increase with n_2. The section of results (particularly Table 1) shall exemplify these conclusions. Lastly and most importantly, the exact form of Eq. (12) (by way of Eq. (13)) lends authenticity to the upcoming result that under a certain condition, and contrary to the common notion, the WM function does possess spatial or temporal derivatives.

3. Nondifferentiability when $n_2 \rightarrow \infty$

Noted in Ref. [11], the Weierstrass function "although continuous everywhere is differentiable nowhere." Similar statements can be found elsewhere, e.g., in Ref. [10]. Also stated in [11] is that for the restrictions on γ and D, the series for $z(t)$ converges but the series for $dz(t)/dt$ does not (staying true to the use of time in Ref. [11]). Such statements may deter the use of the derivatives of the WM function. It is clear, however, that for each fixed finite value of n_2, the function $z(x)$ is differentiable, simply because it is a sum of finitely many terms ($n_2 - (n_1 - 1)$ to be precise), each of which is differentiable. It is only for $n_2 \rightarrow \infty$ that the WM function is not differentiable. To understand that, derivatives of the WM function, Eq. (3), are taken. Hence,

$$z(x) = G^{D-1} \sum_{n=n_1}^{n_2} \gamma^{(D-2)n} \cos\left[(2\pi)^q \gamma^n x \right]$$

$$z'(x) = -G^{D-1} \sum_{n=n_1}^{n_2} (2\pi)^q \gamma^{(D-1)n} \sin\left[(2\pi)^q \gamma^n x \right] \qquad (14)$$

$$z''(x) = -G^{D-1} \sum_{n=n_1}^{n_2} (2\pi)^{2q} \gamma^{nD} \cos\left[(2\pi)^q \gamma^n x \right]$$

Regardless of the switch q, as the harmonic functions can only vary between $+/- 1$, they are being multiplied by varying coefficients, $\gamma^{(D-2)n}$, $\gamma^{(D-1)n}$, and γ^{nD}. Under the restrictions of, $n \geq 0$, $1<D<2$ and $\gamma >1$, clearly the first coefficient diminishes with n, while the other two coefficients exponentially increase with n, and rather hastily (graphs of the coefficients as functions of n shall reveal that straightforwardly). Hence, $z(x)$ converges to a certain value by letting n_2 take on a sufficiently large value, which obviously includes $n_2 \rightarrow \infty$. Conversely, $z'(x)$ and $z''(x)$ do not converge under the same conditions. The larger the n_2 value, the larger are both $z'(x)$ and $z''(x)$, at any given x.

However, convergence and differentiability are two different mathematical concepts. Nondifferentiability of the Weierstrass function has intrigued many, starting with Reimann in 1861, as discussed by Ullrich [13]. Perhaps a decisive proof of nondifferentiability of the Weierstrass function is given by Hardy [14] (see also Johnsen [15]). In essence, when $n_2 \rightarrow \infty$ the derivative about any x_0,

$$\lim_{x \to x_0} \frac{z(x) - z(x_0)}{x - x_0} = \lim_{\Delta x \to 0} \frac{\Delta z}{\Delta x} \qquad (15)$$

does not exist, as it has no limit, which can be explained physically. The terms in the sum of $z(x)$, being a self-affine function, tend endlessly smaller, even smaller than any small Δz over any small Δx. That is, $z(x)$ perpetually and successively is being disturbed by the "fractal roughness," so there is never a convergent tangent line.

4. Differentiability when n_2=finite

Of course, letting $n_2 \rightarrow \infty$ is a theoretical case that implies that scales are reduced endlessly, smaller than atomic, quarks, or even Planck scales. Obviously, for practical cases, $n_2 = finite$. Not only that is a physical requirement, it is also a computational requirement, as functions summed to infinity cannot be accommodated computationally. Hence, Eqs. (1-3) are truncated at some finite n_2. When that happens the "fractal roughness" *seizes* at some scale as dictated by n_2, and expressions for *derivatives do exist*. That can be understood rather simply by observing that any single term, *n*, in the Weierstrass function has a well-defined finite derivative. That thought can be extended to two terms by letting $n_2= n_1+1$, so that their sum shall also have well-defined finite derivatives, etc. Hence, for any $n_2=n_1+\Delta n$, where *Δn* is finite, there shall be well-defined first, second, and higher finite derivatives. Under these conditions the derivatives in Eq. (14) are deterministically exact.

Theoretically n_1 and n_2 can take on any finite integer values, with only the trivial restriction that $n_1 < n_2$. However, it is well documented in Ref. [10] that n_1 and n_2 are related to the largest and smallest (finest) scales of the problem at hand. The signal, *z(x)*, would respectively appear "*smooth*" or "*rough*" depending on how "*small*" or how "*large*" are n_1 and n_2. Their selection is detailed in the following sections. Herein, it is assumed that $0 \leq n_1$, where specifically all results reported later are carried out with $n_1=0$.

4.1 Exact calculation of the spectral moments in the spatial domain (n_2=finite)

The exact representation of the WM function and its derivatives allows us to exactly calculate the spectral moments over the spatial range $x \in [0, x_{max}]$. The spectral moments for a continuous waveform are calculated using a continuous (integral) form of their definitions:

$$m_0 = \frac{1}{x_{max}} \int_0^{x_{max}} [z(x)]^2 dx$$

$$m_2 = \frac{1}{x_{max}} \int_0^{x_{max}} [z'(x)]^2 dx \qquad (16)$$

$$m_4 = \frac{1}{x_{max}} \int_0^{x_{max}} [z''(x)]^2 dx$$

While those integrations may seem cumbersome, a symbolic package such as Mathematica can render *exact* solutions (and values) reasonably quickly, using the following script:

9

$$L = 20 * xmax;$$
$$z[x\_] := G^{\wedge}(D-1)*$$
$$\quad Sum\left[Cos\left[(2*Pi)^{\wedge}q*(g^{\wedge}n)*(x) \right] / g^{\wedge}(n*(2-D)), \{n, n1, n2\} \right] // Expand;$$
$$avg = (1/L)*Integrate[z[x+L0] // Expand, x, 0, L]; \qquad (17)$$
$$m0 = (1/L)*Integrate[(z[x+L0] - avg)^2 // Expand, x, 0, L];$$
$$m2 = (1/L)*Integrate[D[z[x+L0], x]^2 // Expand, x, 0, L];$$
$$m4 = (1/L)*Integrate[D[z[x+L0], x, 2]^2 // Expand, x, 0, L];$$

It is *particularly* stressed that the two Mathematica operators *D[z[x],x]*, and *D[z[x],x,2]* produce *analytically exact* first and second derivatives of *z(x)* with respect to *x*, respectively. These match *identically* the derivatives in Eqs. (14). Then note that an (arbitrary) shift *L0* is added to the script to *optionally* remove a certain transient characteristic of *z(x)* near $x=0^+$. Suppose first that there is no shift, i.e., *L0=0* as Eqs. (14) imply. In the region where *x* is "small," the value of $\gamma^n x$ is small too, and the frequency altering effect upon the cosine function is likewise small. Hence, when *L0=0*, the signal *z(x=0)* starts at a relatively high value of

$$z(0) = G^{D-1} \sum_{n=n_1}^{n_2} \gamma^{(D-2)n}$$

Then $z(x=0^+)$ decays rather slowly before the full fractal behavior ensues. And, the decay slows yet with smaller γ. That transient behavior is evident in Fig. 1, which shows the WM function for *G=1, D=1.5, n_1=0*, and *n_2=26,* in the range $0 \le x \le 20$, for three values of for $\gamma = \{1.15, 1.5, 1.85\}$. The insets magnify the signal behavior, shown in red, in the range $0 \le x \le 1m$, i.e., near $x=0^+$. It is also evident that if γ is also small, then $\gamma^n x$ stays small longer yet, and the transient appears more like a single-frequency harmonic function (see especially the case for $\gamma = 1.15$). Had the calculation of the spectral moments been restricted to a signal in that limited range of $0 \le x \le 1$, wrong results would have emerged because the transient behavior would dominate over a significant portion of that limited range, $0 \le x \le 1$.

Hence, two methods are proposed to mitigate that effect: (1) the information from the WM function can be taken to start at some (arbitrary shift) *L0* and onwards, i.e., *L0<x*, or (2) a sufficiently large signal range can be assigned so that the transient behavior about $x=0^+$ is allowed to completely decay, and its overall effect is diminished when equations (16) are calculated by the code in (17). Recall also that Eq. (12) is derived for a signal length, $L \to \infty$, so for equitable comparison, *L* has to be sufficiently large. In the current work, only the latter method is used, where all results herein are reported for *L0=0*, while ensuring a large enough $L=20x_{max}$ for $\gamma = 1.5$ and above, and up to $L=60x_{max}$ for a smaller γ, e.g. $\gamma = 1.15$. In all cases herein $x_{max}=1m$. It should be noted that this transient behavior, shown in Fig. 1, is not specific just to the aforementioned parameters – this behavior is prevalent in all cases summarized in Table 1, which will be discussed later in detail.
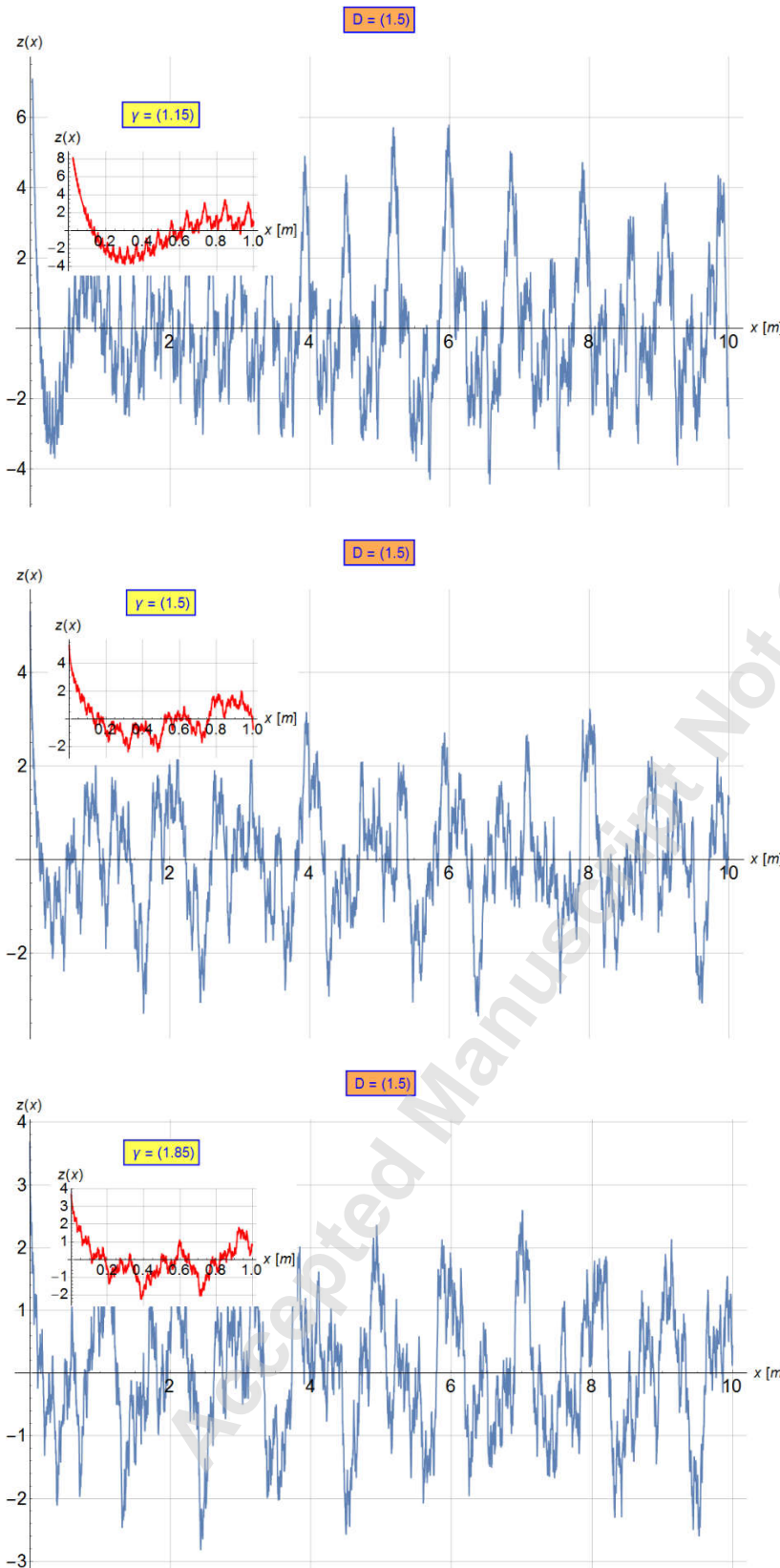
Figure 1. The WM function for $\gamma = \{1.15, 1.5, 1.85\}$, $D=1.5$, $G=1$, $q=1$, $L0=0$, and magnifications at $x \in [0,1]$.

11

It is interesting to note in Fig. 1 that for three cases of $D=1.5$, a "global" harmonic behavior is apparent, which is disturbed by "local" higher frequencies, as γ increases.

Next it should be noted that when n_1 and n_2 are finite, the numerical computation of the WM function over a finite domain is likely to have small non-zero averages. That average is removed from the calculation of m_0, i.e., the spectral moment, m_0, is the statistical second-central-moment (the other spectral moments are not affected by that average, as it is mathematically removed by differentiation).

As discussed previously, the spectral moments can be calculated by the power spectrum. It shall be seen, however, that the moments as reported by Ref. [10] depend on the selection of low and high cutoff frequencies. While those frequencies are claimed in Ref. [10] to be related to n_1 and n_2, the execution of the code in Eq. (17) is free from such a frequency association or selection (i.e., any n_1 and n_2 can be used). Though, for equitable comparison between the various methods, this work shall also adopt the said association as given by Ref. [10].

Conceptually there is nothing that prohibits the execution of the script in Eq. (17). The sums imply accumulation of terms, having the general forms of $A\sin(ax)\sin(bx)$, and $B\cos(cx)\cos(dx)$, which can be integrated *exactly* by Mathematica (even though that can be a slightly tedious task). While the execution of Eq. (17) is CPU intensive, it is not memory demanding. It is simply a matter of time to let Mathematica finish the computation. On a PC with an 8th generation Intel I7 8650U-1.9GHz, the calculation of Eq. (17) can take from a few seconds to a few minutes, depending on the discretization and how many terms, $\Delta n=n_2-n_1$, are retained in the sum. Numerical quadrature (Simpson, Gaussian, Romberg, etc.) is another alternative that may expedite the calculation somewhat, but that offers only marginal gains because convergence must be enforced (this is a known and crucial issue when numerical quadrature is used for highly oscillatory functions). For a reference case of $G=1$, $D=1.5$, $g=1.5$, $n_1=0$, and $n_2=26$, the CPU time is 37 seconds to produce all three spectral moments *exactly* using the script in Eq. (17). Much larger CPU times are needed for larger discretizations that are necessary as γ decreases.

The calculation of the spectral moments can be greatly expedited (by orders of magnitude) using the upcoming numerical procedure, but that is at the cost of computer memory. If computer memory is available in abundance then the following is the recommended procedure.

4.2 Expedient calculation of the spectral moments in the spatial domain (n_2=finite)

Suppose that $z(x)$ is digitized in the following way: (1) a vector x_i is generated to contain N equidistant values of the coordinate x, (2) then $z(x_i)$, $z'(x_i)$, and $z''(x_i)$ are calculated by using Eq. (14). That is, the WM and its derivatives are calculated by the *exact* formulae at locations x_i. (This is distinguished from using numerical derivative calculations, say by finite differences as suggested in Ref. [3], which are *not* used in this work *at all*.) The spectral moments expressed in Eq. (16) can be equivalently obtained in the spatial domain by

$$m_0 = \frac{1}{N}\sum_{i=1}^{N}(z)_i^2 \tag{18}$$

$$m_2 = \frac{1}{N}\sum_{i=1}^{N}(\frac{dz}{dx})_i^2 \tag{19}$$

$$m_4 = \frac{1}{N}\sum_{i=1}^{N}(\frac{d^2z}{dx^2})_i^2 \tag{20}$$

It is again emphasized that this procedure is still considered *exact* because the derivatives are calculated using the exact forms given by Eqs. (16). However, values may slightly differ numerically from the procedure laid out above in Eq. (17), by tiny round-off errors. From a practical point of view, the results are considered to be identical.

Hence, the WM function is equidistantly discretized over the spatial range $x \in [0, x_{max}]$. The values of n_1, and n_2 must be selected to match the problem at hand. As detailed in Ref. [10] they are, respectively, related to the largest scale (say, x_{max}), and the finest resolution (i.e., the highest frequency) capability of the measuring equipment. Correspondingly[3]

$$\begin{aligned} n_1 &= Floor[\ln(1/x_{max})/\ln\gamma + 0.5] \\ n_2 &= Floor[\ln(1/\delta x)/\ln\gamma + 0.5] \end{aligned} \tag{21}$$

While the input parameter x_{max} is independent, the resolution δx depends on the number of discretization points, $n_x = N$. A parameter $nfft$[4] is used to decide the magnitude of n_x according to

$$n_x = 2^{nfft} + 1; \quad \delta x = x_{max}/(n_x - 1) \tag{22}$$

It is that δx value that is used in Eq. (21) to calculate n_2.

Appendix A provides a Mathematica script annotated with comments. That script completely calculates all three spectral moments. The advantage in that script is that the time-consuming integrations are bypassed, and summations are used instead, as implied by Eqs. (18)-(20). But more so, it is recognized that the sum of squared elements in a vector (e.g. Eq. (18)), is entirely equivalent to the execution of the dot-product of that vector with itself. Hence, Eqs. (18)-(20) are completely executed by these pseudo commands

$$\begin{aligned} m_0 &= z.z/N \\ m_2 &= z'.z'/N \\ m_4 &= z''.z''/N \end{aligned} \tag{23}$$

---

[3] In Mathematica's syntax the function *Floor[x+0.5]* rounds to the nearest integer of *x*.

[4] The use of *nfft* in the form of Eq. (22) allows the execution of fast Fourier transforms (FFT), which is set for execution in subsequent works. Otherwise that choice is as good as any.

13

It should be noted that dot-products are highly optimized in modern computer languages, and they can easily be parallelized using multiple cores and threads. Mathematica has both direct access and extensions of the Basic Linear Algebra Subroutines (BLAS) library, which provides a significant performance boost.

On the said computer, even when x_i has over 20 million digitized points, the said Mathematica script renders all three spectral moments in just a few seconds. Clearly this procedure is memory intensive. Computer memory of 16 GB is found mostly sufficient to execute the procedure for up to *nfft=20* in some cases. Unlike the procedure outlined above in Eq. (17), which is restricted to an analytical function, the procedure outlined in Eq. (23) is *valid for any digitized signal*, whether it originates from an analytical function or from experimental data (for the latter, procedures to calculate derivatives are of course needed).

Consider again the case listed above of *G=1, D=1.5, g=1.5, n_1=0, n_2=26*, and *n_x= 655,361*. On the said computer, the CPU time to execute all three terms in Eq. (23) is only 2 seconds, i.e., it is 17 times faster than the previous procedure of Eq. (17). In some cases, the speed-up is more than 60-fold. In all cases that are reported in Table 1, the final results calculated from Eqs. (13), (17), and (23) are *practically indistinguishable* (the difference is caused by merely numerical round-off errors).

By not recognizing the dot-product character when programming Eqs. (18)-(20) (i.e., squaring each element in the sums individually, then totaling (summing) up, and dividing by N to average), the calculations may require much greater CPU times. That mitigates the effectiveness and the advantage of the discretization (or digitization). That increase in CPU time happens only when *nfft* is rather large (*nfft=20* is very large in that regard). For lower values of *nfft*, programming Eqs. (18)-(20) as they appear has shown to still provide significant CPU time savings compared to the procedure in Eq. (17), but it is never better than using the dot-product as outlined in Eq. (23). It should be noted that Mathematica (as executed herein) is used in its normal interpreted mode, so execution is relatively slow. Had this been implemented in a compiled language (e.g., Fortran, C++, etc.) execution times would be much faster (likely near zero or indistinguishably from zero CPU times, in most cases).

In this work, the emphasis is on data reduction of rough surfaces, which particularly have fractal roughness. This is for the purpose of contact mechanics modeling (e.g., applying the venerable Greenwood-Williamson (GW) model [1]). However, the above numerical concepts and procedures apply equally well to the processing of *any digitized signal* that does not necessarily originate from a fractal function (e.g., real surface measurements).

5. Results

Starting with the most important conclusion up front: Eqs. (12), (16, 18-20), and (23) all produce *identical* spectral moments, when implemented respectively by Eqs. (13), (17), and (24). As

14

these equations are founded on different mathematical concepts, they imply that the WM function does possess finite derivatives when n_2 is *finite.* The equations provided by Majumdar and Tien [10] for the same (i.e., Eq. (8)) exhibit enormous errors, and they are untrustworthy. The details are as follows.

First it is noted that the "fractal roughness," G, appearing in Eqs. (1)-(3), is just a constant that provides a global scale for the WM function. Otherwise, it has no role (and perhaps that is the reason Berry and Lewis [11] ignore it altogether). It is therefore assigned here the value of unity, $G=1$. Any other G value would have just scaled equally all spectral moments, but not the relative standing between them. Secondly, for all cases studied here, $q=1$, $n_1=0$, making $f_l=1$ *cycles/m* (or *Hz*), and $\omega_l=2\pi$ *rad/m* (or *rad/s*). The signal length is $x_{max}=1$ *m*. The parameter *nfft* takes on values of {10, 15, 20} to provide respectively signals of different resolution scales according to Eq. (22) of $\delta x=\{976, 30.5, 0.954\}$ *μm*, which are spread over different orders of magnitude. These values of δx, along with the parameter γ allow the calculation of n_2 according to Eq. (21), and then the calculation of ω_h and f_h according to Eq. (9). All these parameters are given in Table 1 along with the outcome of the calculations.

The values of D and γ are clearly independent (and physically they have different meaning). But they are of the same order of magnitude. Hence, for the first batch of comparisons these are made to equal each other (to reduce the number of comparisons), and for the second batch they are made different from each other. To cut in the amount of numerical data reporting, the following is an error analysis between Eqs. (12), (16, 18-20), and (23). The relative errors are defined according to

$$\text{error} = \text{abs}(value_{Eq.(13)} - value_{another\ Eq.}) / value_{Eq.(13)}$$

Indeed, the results from Eq. (13) are regarded exact, where all other results are compared relatively to those. The other equations compared are (8), (17) and (23, 24). A global summary of all errors is also given in Table 1.

First, the errors from Eqs. (17), and (24) are analyzed. As seen from Table 1, the maximum error between *all* the m_0 values is 0.12%, the minimum is 0%, the average 0.06% and the standard deviation is 0.04%. These are indeed very small errors. The spectral moments m_2 and m_4 show even smaller errors. It is concluded the Eqs. (12), (16, 18-20), and (23), as implemented by Eqs. (13), (17), and (24) practically render identical results. So, it is sufficient to use only the results from Eq. (13), as it originates from an *exact* derivation anyway.

The nearly identical values between Eqs. (12), (16, 18-20), and (23), reaffirms that the WM does have finite derivatives when $n_2 = finite$, because otherwise such close matches would not have been at all possible. Moreover, the moment m_0, as it appears in Eqs. (16), (18), and (23), in the spatial domain, is free from any derivatives. Hence, the values calculated by these equations are

15

undisputed. Yet, all these render values that agree with Eq. (12), which stems from a spectral approach. These observations reinforce the analyses and methods presented in this work.

Now a comparison between Eqs. (8) and (13) shows that the errors in the spectral moments as derived in Ref. [10] are huge, rendering those untrustworthy. As seen from Table 1, the maximum error between *all* the m_k values is about 96%; the minimum ranges from 46% to 70%, the average is greater than 80% and the standard deviation ranges from 8% to 19%. The reason for such enormous errors is that the spectral moments produced in Ref. [10] are based upon an approximated power spectrum derived in Ref. [11]. That raises the question of whether the power-law approximated spectrum of Eq. (7), can be regarded as a true representation of the actual spectrum, Eq. (6).

Within each group where D and γ have the same values, it is easily seen that m_0 converges with an increase in n_2 (practically all having nearly the same values), while m_2 and m_4 clearly diverge rather hastily with an increase in n_2, or a decrease in the resolution, δx. This is consistent with the discussion and predictions given above in the mathematical derivation sections. This, of course, prompts the question and the challenge of how (if not whether) these moments can be used in the calculation of the parameters necessary for the GW model [1].

The CPU times shown in Table 1 pertain only to Eq. (17), but the CPU times to calculate the other equations are zero for Eqs. (13), and (8), as these are analytical and have closed-form equations. The CPU times are negligible for Eq. (24), when computer memory is sufficiently available. As *nfft* or n_2 become larger, the CPU times grow larger. Still these are reasonably small, where a few minutes of CPU time at most, will eventually calculate the spectral model even for very large *nfft* or n_2 parameters.

6. Conclusions

The upside of the GW model is that only three spectral moments are needed to execute it. That is also the downside of the GW model, as only a few parameters are available to work with. To estimate the spectral moments reliably, the surface roughness needs to undergo a massive data reduction with very little room for error. In that regard, the current work produces *exact* equations for the calculation of spectral moments for WM fractal function. Spectral moments stemming from previous works, e.g., Ref. [10], are shown to contain enormous errors. These are caused by the approximated (i.e., inexact) power spectrum given in Ref. [11].

The derivation of the spectral moments in the spectral domain and in the spatial or temporal domains are entirely disjointed mathematically. That is, in the former, the spectral moment derived are independent of, and thus relieved from, any derivatives of the WM function. Yet, the very same spectral moments, specifically those calculated in the spatial domain that do depend on such derivatives, produce practically identical results. That supports the fact that derivatives for the WM fractal function do exist when $n_2 = finite$.

16

While most of the work is dedicated to the analytical treatment of the WM function, the numerical procedures presented herein can be easily tweaked to suit other functions or digitized data stemming from real surface measurements. In particular, the dot-products as suggested by Eq. (23), and implemented in Eq. (24), have proven to deliver substantial computational savings while maintaining fidelity.

17

Table 1 Spectral moments and error analyses $\left(g \equiv \gamma;\ delx \equiv \delta x \right)$, for $G=1$, $n_1=0$, and $f_l=1Hz$, $q=1$.

Input	Parameters				Eq. (13), Eq. (17), or Eq. (24)				Eq. (8), same as in Ref. [10]		
	nfft	n2	fh[kHz]	delx(um)	m0	m2	m4	CPU	m0	m2	m4
g=D=1.15	10	50	1.083	976	2.364	3.45E+03	2.71E+10	115	0.093	1.48E+02	1.02E+09
g=D=1.15	15	74	31.02	30.5	2.364	1.02E+04	6.07E+13	262	0.093	4.40E+02	2.28E+12
g=D=1.15	20	99	1021.1	0.954	2.364	3.01E+04	1.88E+17	586	0.093	1.29E+03	7.06E+15
g=D=1.5	10	17	0.985	976	1.499	5.83E+04	1.06E+12	19	0.196	7.63E+03	9.75E+10
g=D=1.5	15	26	37.88	30.5	1.500	2.24E+06	6.02E+16	37	0.196	2.93E+05	5.54E+15
g=D=1.5	20	34	970.7	0.954	1.500	5.75E+07	1.01E+21	84	0.196	7.52E+06	9.33E+19
g=D=1.85	10	11	0.869	976	2.643	3.02E+06	6.50E+13	9	1.356	1.08E+06	1.48E+13
g=D=1.85	15	17	34.8	30.5	2.860	1.60E+09	5.54E+19	21	1.493	5.72E+08	1.26E+19
g=D=1.85	20	23	1396.2	0.954	2.932	8.51E+11	4.73E+25	53	1.539	3.04E+11	1.07E+25
D=1.5											
g=1.15	10	50	1.083	976	3.830	1.64E+05	2.90E+12	119	0.569	2.43E+04	3.76E+11
g=1.5	10	17	0.985	976	1.499	5.83E+04	1.06E+12	19	0.196	7.63E+03	9.75E+10
g=1.85	10	11	0.869	976	1.088	3.73E+04	6.07E+11	7	0.129	4.43E+03	4.41E+10
g=3.0	10	6	0.729	976	0.750	2.16E+04	3.14E+11	4	0.072	2.08E+03	1.46E+10
g=3.0	20	13	1594	0.954	0.750	4.72E+07	3.28E+21	31	0.072	4.56E+06	1.53E+20
g=1.5											
D=1.15	10	17	0.985	976	1.004	1.21E+03	9.86E+09	16	0.032	4.93E+01	2.82E+08
D=1.5	10	17	0.985	976	1.499	5.83E+04	1.06E+12	19	0.196	7.63E+03	9.75E+10
D=1.85	10	17	0.985	976	3.877	4.86E+06	1.20E+14	18	2.069	2.03E+06	3.57E+13
D=1.85	20	34	970.74	0.954	4.304	5.97E+11	1.42E+25	89	2.33	2.49E+11	4.25E+24
		Max.	Error		0.12%	0.03%	0.00%		96.82%	95.93%	97.14%
		Min.	Error		0%	0%	0.00%		46.63%	58.37%	70.16%
		Average	Error		0.06%	0.00%	0.00%		80.25%	83.69%	88.96%
		St. Dev.	Error		0.04%	0.01%	0.00%		19.02%	12.55%	8.31%

7. Appendix A

The script below, in Eq. (24), is annotated with Mathematica (* comments *). It provides a complete procedure to calculate all spectral moments based on Eq. (23). The advantage here is that the integrations are bypassed, and dot-products are used instead of summations as implied by Eqs. (18)-(20). Hence, the Mathematica code is:

$nfft = 10;$

$nx = 2^{\wedge} nfft + 1; \quad delx = L / (nx - 1);$

(* digitize the signal, start at L0, go to L+L0, in increments of delx *)

$x0 = Table[x, \{x, L0, LL + L0, delx\}];$ (* vector containing the delx-spaced, x-coord.*)

$N0 = Length[x0];$

$ravg = Total[z[x] /. x \rightarrow x0] / N0;$ (* sub. x0 into WM func., Eq. (17), calc. the average *)

$r = z[x] - ravg;$ (* remove the average from the WM function, Eq. (17) *)

$tmp = r /. x \rightarrow x0;$ (* digitize r; and assign it to a temporary vector tmp *)

$m0 = tmp.tmp / N0;$ (* dot-product, averaged; this is the zeroth spectral moment *)

$rd = D[z[x], x];$ (* 1st derivative of z[x]; the derivative is exact! See Eq. (14) *)

$tmp = rd /. x \rightarrow x0;$ (* 1st derivative digitized; assign to tmp *)

$m2 = tmp.tmp / N0;$ (* dot-product, averaged; the second spectral moment *)

$rdd = D[rd, x];$ (* 2nd derivative of z[x]; the derivative is exact! See Eq. (14) *)

$tmp = rdd /. x \rightarrow x0;$ (* 2nd derivative digitized; assign to tmp *)

$m4 = tmp.tmp / N0;$ (* dot-product, averaged; the fourth spectral moment *) $\qquad$ (24)

8. References

[1] Greenwood J. A., and Williamson J. B. P., 1966, "Contact of Nominally Flat Surfaces," Proceedings of the Royal Society of London. Series A. Mathematical and Physical Sciences, **295**(1442), pp. 300–319.

[2] McCool, J. I., 1987, "Relating Profile Instrument Measurements to the Functional Performance of Rough Surfaces," Journal of Tribology, **109**(2), p. 264.

[3] McCool, J. I., 1982, "Finite Difference Spectral Moment Estimation for Profiles the Effect of Sample Spacing and Quantization Error," Precision Engineering, **4**(4), pp. 181–184.

[4] Bendat, J. S., and Piersol, A. G., 1966, *Measurement and Analysis of Random Data*, Wiley, New York, NY.

[5] Bendat, J. S., and Piersol, A. G., 1980, *Engineering Applications of Correlation and Spectral Analysis*, John Wiley and Sons, Inc., New York.

[6] Bendat, J. S., and Piersol, A. G., 2011, *Random Data: Analysis and Measurement Procedures*, John Wiley & Sons.

[7] Brown, S. R., 1995, "Simple Mathematical Model of a Rough Fracture," Journal of Geophysical Research: Solid Earth, **100**(B4), pp. 5941–5952.

[8] Vogel, F., 2001, "Spectral Moments and Linear Models Used for Photoacoustic Detection of Crude Oil in Produced Water," University of Oslo, Department of Informatics.

[9] Sweitzer, K., Bishop, N., and Genberg, V., "Efficient Computation of Spectral Moments for Determination of Random Response Statistics," p. 17.

[10] Majumdar, A., and Tien, C. L., 1990, "Fractal Characterization and Simulation of Rough Surfaces," Wear, **136**(2), pp. 313–327.

[11] Berry, M. V., and Lewis, Z. V., 1980, "On the Weierstrass-Mandelbrot Fractal Function," Proceedings of the Royal Society A: Mathematical, Physical and Engineering Sciences, **370**(1743), pp. 459–484.

[12] Davidson, K. L., and Loughlin, P. J., 2000, "Instantaneous Spectral Moments," Journal of the Franklin Institute, 337(4):421-436. 10.1016/S0016-0032(00)00034-X.

[13] Ullrich, P., 1997, "Anmerkungen zum "Riemannschen Beispiel einer stetigen, nicht differenzierbaren Funktion," Results. Math., **31**(3–4), pp. 245–265.

[14] Hardy, G. H., 1916, "Weierstrass's Non-Differentiable Function," Transactions of the American Mathematical Society, **17**(3), p. 301.

[15] Johnsen, J., 2010, "Simple Proofs of Nowhere-Differentiability for Weierstrass's Function and Cases of Slow Growth," J Fourier Anal Appl, **16**(1), pp. 17–33.